Title

Characterizing the dark state in thymine and uracil by double resonant spectroscopy and quantum computation.

Journal

Physical chemistry chemical physics : PCCP, 17(37)

ISSN

1463-9076

Authors

Ligare, M
Siouri, F
Bludsky, O
et al.

Publication Date

2015-10-01

DOI

10.1039/c5cp03516c

Peer reviewed

PCCP

ARTICLE

Characterizing the dark state in thymine and uracil by double resonant spectroscopy and quantum computation

Received 00th January 20xx,
Accepted 00th January 20xx

DOI: 10.1039/x0xx00000x

www.rsc.org/

M. Ligare,[a] F. Siouri[a], O. Bludsky,[b] D. Nachtigallova,[b*] M.S. de Vries[a*]

We report on gas phase double resonant spectroscopy of both the ground state and the dark excited state in isolated uracil and thymine. We also report lifetimes of the dark state for different excitation wavelengths. In combination with ab initio calculations the results suggest that the dark state is of triplet ($3\pi\pi^*$) character

1.Introduction

The ultra-short excited state lifetimes of isolated nucleic acid bases are a well-known phenomenon which was observed experimentally by several authors, both in the gas phase and in solution[1-4]. The primary mechanism is identified as subpicosecond internal conversion to the electronic ground state. This process protects the nucleobases from otherwise potentially harmful UV-photochemistry. This property may have played a selective role in prebiotic chemistry on an early earth, considering that many non-canonical derivatives have long excited state lifetimes and that the intrinsic properties of the nucleobases must have been unchanged since their incorporation in the reproductive machinery. It is thus conceivable that the choice of the genetic alphabet was aided by a photochemical selection that preceded any biological evolution. If that is the case, the photochemical properties of the bases are molecular fossils of prebiotic chemistry. However for uracil and thymine the electronic relaxation pathway competes with another, incompletely understood, process which causes a very small fraction of excited molecules to populate a "dark" excited state. Here we report on gas phase spectroscopy probing directly that dark excited state in isolated uracil and thymine. In combination with ab initio calculations, the IR spectra suggest that the dark state is of triplet ($^3\pi\pi^*$) character.

Computational studies show that the rapid relaxation of photoexcited nucleobases to the ground state proceeds through nonadiabatic transitions via conical intersections on the crossing seam of potential energy surfaces of excited and ground states characterized by strongly ring-puckered structures[5-25]. Several conical intersections were found for naturally occurring nucleobases for which efficiencies depend on the reaction paths from the excited state minima to a particular structure on the crossing seam. A comprehensive study performed by Barbatti et. al. shows that the purine bases, guanine and adenine, relax with a single-exponential decay along one excited state potential energy surface (PES) leading directly to the intersection with the ground state PES [26]. However, the pyrimidine-based nucleobases, cytosine, thymine and uracil, exhibit a more complex picture with several excited states involved in the relaxation process. A small portion of excited state molecules appears to populate a "dark state", the character of which has been extensively debated in recent literature. As a result, the UV damage resistance is not complete and the dark state may act as a precursor to formation of photolesions by dimerization of adjacent pyrimidine bases in DNA. For thymine which has the longest excited-state lifetime among the nucleobases, photodynamics simulations show that after excitation to the S_2 state of $\pi\pi^*$ character the system relaxes to the minimum of the S_2 state. Due to the flat character of the PES of this state, the relaxation is delayed. S_2/S_1 intersections then lead to the S_1 state of $n\pi^*$ character where the system is trapped and an additional delay occurs before internal conversion to the ground state. This entire deactivation mechanism still proceeds on a pico-second timescale. However, an additional sub-nanosecond to nanosecond relaxation pathway to a non-fluorescent ("dark") state has been reported in many experimental studies [1, 27, 28]. This state was also observed for methylated derivatives of uracil and thymine [29, 30].

Several candidates for the dark state have been suggested, including the vibrationally "hot" ground state, the S_1 state of $^1(n\pi^*)$ character, and the T_1 state of $^3(\pi\pi^*)$ or $^3(n\pi^*)$ character [27-33]. The involvement of different tautomeric forms of thymine was ruled out by Schultz and co-workers on the basis of theoretical calculations [28]. According to the current understanding of the photophysics of thymine, the $^3(\pi\pi^*)$ state is the most likely candidate. Three possible pathways

[a] Department of Chemistry and Biochemistry. University of California, Santa Barbara, CA 93117-9510. USA.
[b] Institute of Organic Chemistry and Biochemistry v.v.i., AS CR, Flemingovo nam. 2, 16610 Prague, Czech Republic.
* devries@chem.ucsb.edu,
dana.nachtigallova@uochb.cas.cz

Electronic Supplementary Information (ESI) available: Table ST1. Vibrational frequencies of the NH stretching modes of thymine. Table ST2. Vibrational frequencies of the NH stretching modes of uracil. See DOI: 10.1039/x0xx00000x

have been suggested to populate this state from the initially excited $^1(\pi\pi^*)$ state: a direct $^1(\pi\pi^*) \rightarrow {}^3(\pi\pi^*)$ path or one of two indirect pathways: $^1(\pi\pi^*) \rightarrow {}^3(n\pi^*) \rightarrow {}^3(\pi\pi^*)$ or $^1(\pi\pi^*) \rightarrow {}^1(n\pi^*) \rightarrow {}^3(\pi\pi^*)$ [31].

Several authors have interpreted time-resolved pump-probe ionization and vibrational spectra (ref 6-9,12) using excited state calculations. The interpretations are based mainly on characterization of the potential energy surface and the spin-orbit coupling terms [30-32]. Etinski et al. [32] provided support of the triplet state based on the interpretation of time resolved infrared spectra in acetonitrile solution[33], in particular the peak at 1500 cm^{-1}, resulting from a combination of the C4-C5 stretching and the N1H wagging motions, and the peak near 1350 cm^{-1} due to the ring deformation vibration. These authors reported a 560 ns excited state lifetime, attributed to a triplet state.

In this work we propose an assignment of the long-lived dark state, based on NH vibrational frequencies of the dark state, obtained with double resonant IR-UV spectroscopy of excited state uracil and thymine. We interpret these frequencies using computational studies which include analysis of NH frequencies accounting for the anharmonicity effects.

2. Methods

2.1 Experimental

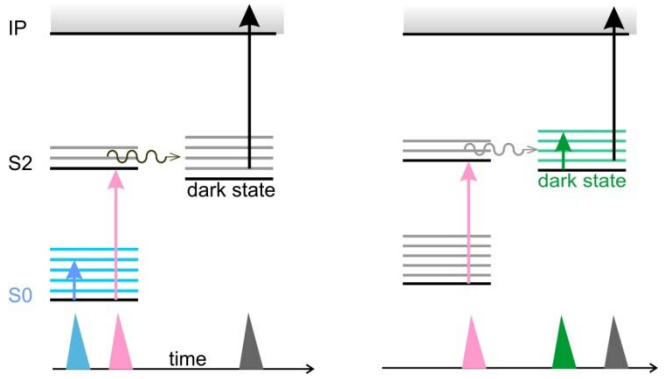

Figure 1: Pulse sequences employed to obtain ground state IR (left) and excited state IR (right panel).

The instrument has been previously described in detail [34]. A brief description of the instrument and experimental setup follows. Samples are placed on a translating graphite substrate directly in front of a pulsed molecular beam valve, based on a piezo cantilever design[35]. They are laser desorbed by a Nd:YAG laser (1064nm, ~1 mJ/cm^2), then entrained in a supersonic molecular beam of argon (6 atm backing pressure). The cold, neutral molecules are ionized by resonance enhanced multiphoton ionization (REMPI) and are subsequently detected by a reflectron time of flight mass spectrometer. For REMPI spectroscopy two lasers are spatially and temporally overlapped. The first and resonant photon comes from the frequency doubled output of a tunable dye laser (Lumonics HD-300) with maximum spectral line width 0.4 cm^{-1} and pulse energy 0.3-0.7 mJ. The second photon comes from an excimer laser (193 nm, 1.5-2 mJ/pulse). A variable delay between dye laser and excimer laser allows measurement of excited state lifetimes. For IR-UV double resonance spectroscopy we use an additional IR laser in two different pulse sequences, depending on whether the ground state or the dark state is probed, shown in Fig. 1 [36-39]. The IR laser is an OPO/OPA (Laser Vision) pumped by a Nd:YAG laser (Quanta Ray DCR-2A, 550 mJ/pulse). The near-IR output has a pulse energy of 3-5 mJ over the range of 3200-3800 cm^{-1} and spectral width of 3 cm^{-1}. The standards for thymine and uracil were purchased from Sigma Aldrich and used without further purification.

2.2 Computational

The minimal structure, harmonic and anharmonic frequencies of the ground and excited states were calculated at the Moller-Plesset perturbation theory (MP2) [40] level and with the second-order algebraic diagrammatic construction (ADC(2)) method [41, 42], with the resolution of identity [43], respectively. The cc-pVTZ basis set [44] was used throughout the calculations. Anharmonic frequency calculations at the second-order perturbation theory (PT2) level were carried out for the ground electronic state using Gaussian09[45]. One-dimensional NH stretching frequencies (1D-scan) were obtained by solving (1) using the Numerov-Cooley integration technique[46].

$$\left\{-\frac{\hbar^2}{2\mu}\frac{\mathrm{d}^2}{\mathrm{d}r_{NH}^2} + V(r_{NH})\right\}\chi_n(r_{NH}) = E_n\chi_n(r_{NH}), \quad (1)$$

where

$$\frac{1}{\mu} = \frac{1}{m_N} + \frac{1}{m_H}$$

and $V(r_{NH})$ is a potential energy surface scan over the N-H bond coordinate. Assuming small coupling of the NH stretching motion with other vibrational degrees of freedom, the 1D-scan results should be comparable to one-dimensional anharmonic frequencies evaluated from diagonal anharmonic constants (denoted as 1D-PT2).

3. Results

UV excitation spectra

Both U and T have broad onsets in the UV, as first reported by Brady et al. [47]. We have now obtained higher resolution two photon spectra of U and T, showing the same onset as reported before, but now also showing some structure as shown in Figure 2. The gradual onset and the absence of a dominant origin peak may indicate a large geometry change between ground state and excited state. The ionization potentials of U and T are 9.60 and 9.20 eV, respectively[48]. These values are more than twice the $S_0 \rightarrow S_2$ excitation energy and thus one-color R2PI does not suffice for ionization. The spectra in Figure 2 result from two-color R2PI with 193 nm as the second color. We observe ions after delaying the second laser pulse by up to several nanoseconds, which we interpret as ionization out of one or more long lived dark states, which we shall denote by S*. It should be noted that these are action

spectra and thus their structure does not necessarily reflect only the absorption characteristics. The ions we detect are those that have arrived in S* on the nanosecond timescale. Spectral features can be due to absorption resonances but they can also result from potential energy surface dependence of the transitions from the excited state to the dark state(s). We will consider possible scenarios for this effect in the discussion section.

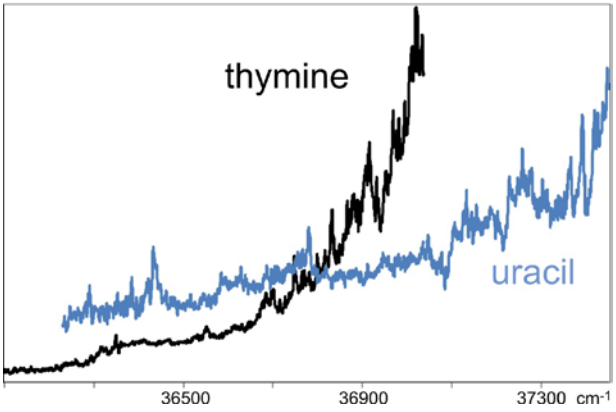

Figure 2: Two-color R2PI spectra of uracil and thymine. The second photon is at 193 nm in both cases.

IR spectra

We have obtained the first gas phase IR spectra for uracil (Fig. 3) and thymine (Fig. 4), both for the ground state and for the dark state. The pulse sequences employed to obtain these spectra appear in Figure 1. For the ground state, an initial IR pulse is scanned in the NH and OH stretch frequency region and followed by two-step ionization probing. When the IR pulse is resonant with a vibrational frequency this modifies the ground state vibrational population producing a modified Franck-Condon landscape. Usually this modification reduces the ion probe signal, but in this case it increases the ion probe signal. This result suggests a strong geometry change between S_0 and S_2, consistent with the gradual onset of the UV absorption. To obtain a zero background gain spectrum the first UV pulse of the two-step ionization probing was set to 35,714 cm^{-1} where no ionization occurs without IR excitation.
For the dark state, the pulse sequence starts with excitation to S_2 (purple pulse, Fig 1) followed by rapid relaxation to the dark state. After 20 ns the IR laser is fired (green pulse) followed after another 30 ns by the ionization pulse from the excimer laser (black pulse), serving as the probe. In this sequence the IR laser modifies the dark state vibrational population, producing the green ion-dip spectra.

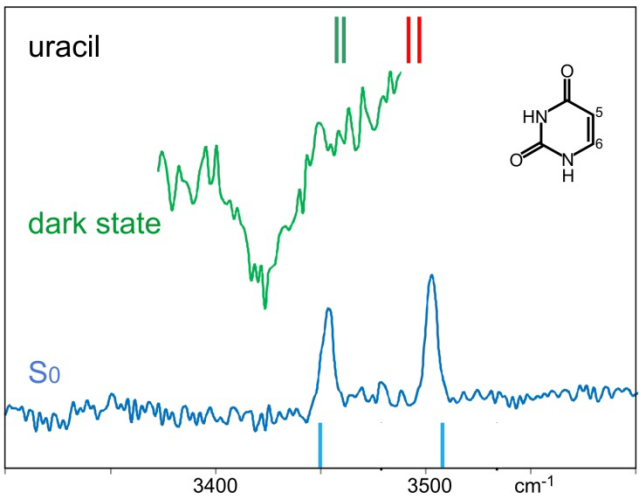

Figure 3: IR-UV double resonant spectra of the ground state (blue) and dark excited state of uracil (green). Computed frequencies of the NH stretches are indicated as stick spectra. The frequencies of S_0 state (blue) are obtained with fully-dimensional anharmonic calculations. The S_1 (red) and T_1 (green) frequencies are estimated from the 1D-scan with the assumption of the same corrections for full anharmonicity as for the S_0 state.

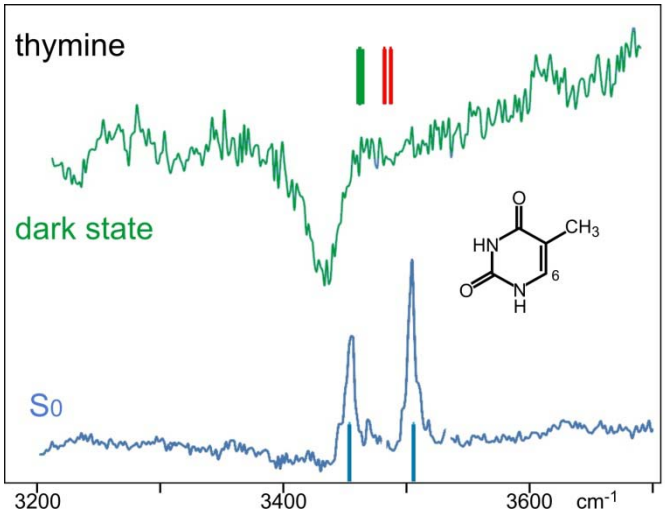

Figure 4: Same data as in Figure 3 for thymine.

Lifetimes

We have obtained lifetimes for the dark state by nanosecond pump probe measurements. We achieve this by varying the delay between the excitation laser pulse and the ionization laser pulse (purple and black in Figure 1). We can fit the decay curves with a single exponential decay plus, in the case of thymine a very long time component. Table 1 lists the lifetimes derived from the single exponential decay fits. For uracil the lifetime varies from 49 to 64 ns, depending on wavelength. For thymine the lifetime is longer and depends more strongly on excitation wavelength, from 220 ns to 293 ns. For thymine we also observe a very long timescale component. We cannot exclude that this component is due to a long lived excited state, but which we interpret it as more likely due to ionization

out of the hot ground state, resulting from the rapid internal conversion out of the ππ* state. This would leave the ground state with about 4.5 eV of internal excitation and a very broad Franck-Condon landscape for photo-ionization. Following the pump pulse, the excited molecules move through the probe laser beam spot of about 3 mm in approximately 6 μs. The long lived signal component decreases on that time scale and this indicates a lifetime longer than our experimental window. This time scale is consistent with a hot ground state with a statistical dissociation rate far exceeding that 6 μs window. Within the signal to noise the signal appears to depend linearly on 193 nm power, indicating a single photon process.

Uracil			Thymine	
λ(cm^{-1})	τ(ns)		λ(cm^{-1})	τ(ns)
37,392	55.2 ± 2		36,364	248 ± 11
37,258	49.5 ± 2		36,748	219 ± 5
37,008	58.6 ± 2		36,917	219 ± 4
36,781	63.9 ± 3		37,012	293 ± 7
36,510	65 ± 8			
36,434	67 ± 3			

Table 1: Excited state lifetimes for U and T obtained at different excitation wavenumbers.

4. Discussion

Ground state

The calculated NH stretching frequencies in the ground state and excited state of thymine and uracil appear in Tables S1 and S2, respectively. We evaluated the anharmonic effects for the NH stretching mode for the ground state, both by employing one-dimensional scans of the NH bond length (1D-scan) and from the diagonal anharmonic constants corresponding to NH stretching modes (1D-PT2).

For both systems the former method gives slightly smaller corrections compared to the 1D-PT2 calculations. The differences are, however, small and justify the reliability of 1D-scan calculations. Both methods yield a blue-shift of about 30 cm^{-1} with respect to the experimentally observed frequencies which are recovered in fully-dimensional anharmonic PT2 calculations. Comparison of the results of PT2 with both 1D-PT2 and 1D-scan indicate a relatively small coupling between NH stretching modes and other degrees of freedom. In addition, these calculations which accounted for full-dimensional anharmonicity provided frequencies in a very good agreement with the experiment, confirming that this is the diketo tautomer as seen in previous experiments [49-54]. The frequencies appear as blue stick spectra in Figures 3 and 4.

Dark state

To interpret the dark state IR spectra, we performed calculations for both the S_1 and T_1 states. The resulting NH vibrational frequencies for S_1 are nearly degenerate with a splitting of 5 cm^{-1} for both species. The S_1 frequencies obtained with 1D-scan corrections show blue shifts of 29/34 cm^{-1} and 35/40 cm^{-1} with respect to the lower-energy frequency of the ground states of thymine and uracil, respectively, shown in red in Figs 3 and 4. Because of the structural similarities at the S_1 and S_0 minima, the effects of anharmonicity may be expected to be similar and, thus, the full-dimensional anharmonic calculations are expected to give very similar effects for S_1 and S_0. Based on these assumptions, the frequencies corresponding to the S_1 state are predicted to fall in the range of 3480-3490 cm^{-1}, i.e. blue-shifted from the lower NH stretching band by about 30 – 40 cm^{-1}.

As in the case of the S_1 minima, the calculations performed for the T_1 minima predict only small splittings of the NH frequencies of 1 and 3 cm^{-1} for thymine and uracil, respectively. The calculated shifts with respect to the lower-energy NH frequencies of the ground states are significantly smaller for the T_1 state, at 8 and 9 cm^{-1} and 2 and 5 cm^{-1} for thymine and uracil, respectively (in green in Figs. 3 and 4). In addition to the global minimum structures of the triplet states, we also investigated the local excited state minima characterized by planar structures. The corresponding NH frequencies are shifted to higher energies with respect to the lower-energy NH vibrations of the ground states by 23 and 26 cm-1 for thymine and 30 cm-1 for uracil, respectively. These structures are energetically separated from their corresponding global minima by 3.65 and 2.69 kcal/mol in the case of thymine and uracil, respectively.

The prediction of the position of the NH stretching band of the S_1 state, made with the assumption of similar effects of anharmonicity as calculated for the S_0 state, indicate that the observed spectra of both species correspond more likely to the T_1 rather than S_1 states.

We also need to consider the possibility of photo-tautomerization to an enol excited state, which would exhibit a single N-H mode. However, in that case there would be an O-H stretch in the 3600-3700 cm^{-1} range, which we do not observe.

Excited state dynamics.

We postulate that the wavelength dependence of the dark state lifetime reflects the de-excitation dynamics because the S* internal energy depends on the initial excitation to S_2. This model is further supported by the observation that preceding the UV excitation with an IR excitation modifies the measured dark state lifetime. Figure 5 illustrates this observation. Pump-probe data at 37,012 cm^{-1} pump and 193 nm probe wavelengths yields a 293 ns lifetime. Preceding the sequence with an IR pulse at 3504.7 cm^{-1} shortens the lifetime to 164 ns. Both traces, in addition to single exponential decay, have a second lifetime component as well of at least 6 microseconds, which we attributed to ionization out of the hot ground state, following direct internal conversion from S_2. Because of the jet cooling in the molecular beam the molecules all start out in v=0 in the ground state. The IR pulse excites to an NH stretching mode, followed immediately by internal vibrational redistribution to lower frequency modes. In other words, the

IR pulse alters the ground state vibrational distribution, resulting in a different S_2 excited state distribution. These data thus suggest that the ensuing excited state dynamics is sensitive to this excited state distribution and affects the population of the dark state. The dark state signal is both increased and shows a shorter lifetime. Although we can fit this decay with a single exponential, it is of course possible that multiple decay paths contribute.

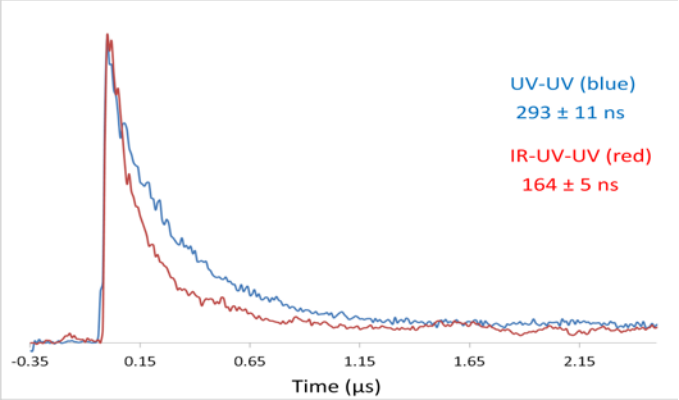

Figure 5: pump probe spectra for thymine with (red) and without (blue) preceding IR excitation. UV pump wavelength is37,012 cm^{-1}, UV probe wavelength is 193 nm. IR excitation at 3504.7 cm^{-1}.

In agreement with previously reported studies on thymine and uracil, the minima of the S_1 states of both species are of $n\pi^*$ character with almost planar structure, similar to the ground state minima. The minima of S_2 are characterized by a distortion from planarity with pyramidalization at the C6 atom [10, 55-58]. The triplet state minima are of $\pi\pi^*$ character and they are also characterized by pyramidalization of the pyrimidine ring at the C6 atom. Therefore, contrary to the S_1 state, more complex behavior is expected for the T_1 state where the distorted global minimum structures are separated by small barriers from the planar structures. One possible consequence could be dependence of the S_2-S* coupling on vibrational modes, with enhancement of the interaction in the case of out-of plane vibrational modes that correspond to pyramidalized structures.

These barriers could also be responsible for the discrepancy between the experimentally observed and calculated spectral shifts between the S_0 and T_1 states. In particular, the assumption of the same corrections for fully-dimensional anharmonicity as used for S_0 and S_1 states predicts blue shifts of about 9 and 5 cm^{-1} for thymine and uracil, respectively, while we observe small red-shifts of about 10 (thymine) and 20 (uracil) cm^{-1} experimentally. Due to the complexity of the vibrational dynamics in T_1 states, the low energy vibrations are expected to further influence the coupling with NH stretching modes.

Figure 6 shows a schematic Jablonski diagram, summarizing our current understanding of the excited state dynamics. A more detailed study of this coupling and further computational modelling using these data may shed further light on the detailed dynamics and this work is currently under way.

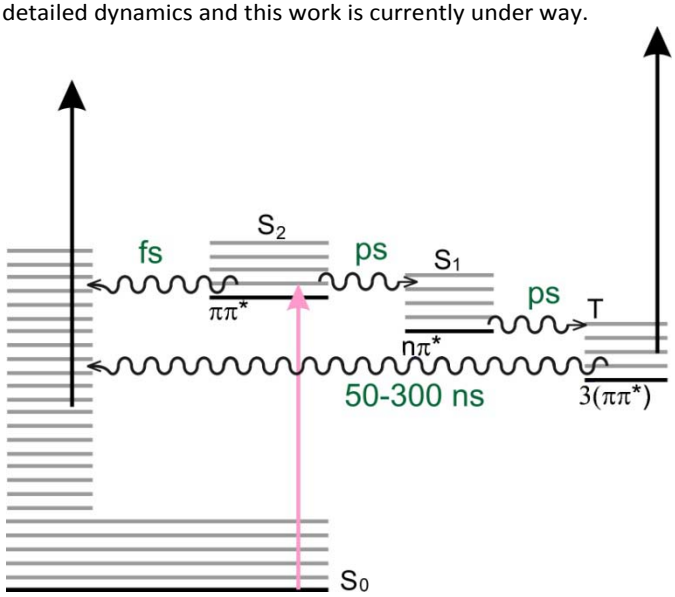

Figure 6: Schematic Jablonski diagram of the processes following UV excitation in thymine and uracil

Acknowledgements

This material is based upon work supported by the National Science Foundation under CHE--1301305 and by NASA under Grant No. NNX12AG77. D.N. acknowledges the funding of the Grant Agency of the Czech Republic (P208/12/1318). The research at IOCB was a part of the project RVO:61388963.

Notes and references

1 H. Kang, K. T. Lee, B. Jung, Y. J. Ko and S. K. Kim, *J. Am. Chem. Soc.*, 2002, 124, 12958-12959.
2 S. Ullrich, T. Schultz, M. Z. Zgierski and A. Stolow, *PCCP*, 2004, 6, 2796-2801.
3 C. Canuel, M. Mons, F. Piuzzi, B. Tardivel, I. Dimicoli and M. Elhanine, *J. Chem. Phys.*, 2005, 122, 074316-074317.
4 P. M. Hare, C. E. Crespo-Hernandez and B. Kohler, *Proceedings of the National Academy of Sciences of the United States of America*, 2007, 104, 435-440.
5 H. R. Hudock, B. G. Levine, A. L. Thompson, H. Satzger, D. Townsend, N. Gador, S. Ullrich, A. Stolow and T. J. Martinez, *J. Phys. Chem. A.*, 2007, 111, 8500.
6 H. Chen and S. H. Li, *J. Chem. Phys.*, 2006, 124.
7 S. Perun, A. L. Sobolewski and W. Domcke, *J. Phys. Chem. A*, 2006, 110, 13238.
8 S. Perun, A. L. Sobolewski and W. Domcke, *J. Am. Chem. Soc.*, 2005, 127, 6257-6265.
9 L. Serrano-Andres, M. Merchan and A. C. Borin, *Proceedings of the National Academy of Sciences of the United States of America*, 2006, 103, 8691-8696.
10 S. Matsika, *J. Phys. Chem. A*, 2004, 108, 7584-7590.
11 N. Ismail, L. Blancafort, M. Olivucci, B. Kohler and M. A. Robb, *J. Am. Chem. Soc.*, 2002, 124, 6818-6819.

12 A. L. Sobolewski and W. Domcke, *European Physical Journal D*, 2002, 20, 369-374.
13 E. Epifanovsky, K. Kowalski, P. D. Fan, M. Valiev, S. Matsika and A. I. Krylov, *J. Phys. Chem. A*, 2008, 112, 9983-9992.
14 L. Serrano-Andres, M. Merchan and A. C. Borin, *J. Am. Chem. Soc.*, 2008, 130, 2473-2484.
15 S. Perun, A. L. Sobolewski and W. Domcke, *Chem. Phys.*, 2005, 313, 107-112.
16 M. Barbatti and H. Lischka, *J. Am. Chem. Soc.*, 2008, 130, 6831.
17 E. Fabiano and W. Thiel, *J. Phys. Chem. A*, 2008, 112, 6859-6863.
18 C. M. Marian, *J. Phys. Chem. A*, 2007, 111, 1545-1553.
19 Z. G. Lan, E. Fabiano and W. Thiel, *ChemPhysChem*, 2009, 10, 1225-1229.
20 M. Barbatti, J. J. Szymczak, A. J. A. Aquino, D. Nachtigallova and H. Lischka, *J. Chem. Phys.*, 2011, 134, 014304.
21 M. Barbatti, A. J. A. Aquino, J. J. Szymczak, D. Nachtigallova and H. Lischka, *PCCP*, 2011, 13, 6145-6155.
22 K. A. Kistler and S. Matsika, *J. Chem. Phys.*, 2008, 128, 215102-215114.
23 L. Blancafort and M. A. Robb, *J. Phys. Chem. A*, 2004, 108, 10609-10614.
24 A. L. Sobolewski and W. Domcke, *PCCP*, 2004, 6, 2763-2771.
25 M. Z. Zgierski, S. Patchkovskii, T. Fujiwara and E. C. Lim, *J. Phys. Chem. A*, 2005, 109, 9384-9387.
26 M. Barbatti, A. J. A. Aquino, J. J. Szymczak, D. Nachtigallova, P. Hobza and H. Lischka, *Proceedings of the National Academy of Sciences of the United States of America*, 2010, 107, 21453-21458.
27 Y. G. He, C. Y. Wu and W. Kong, *J. Phys. Chem. A*, 2003, 107, 5145-5148.
28 J. Gonzalez-Vazquez, L. Gonzalez, E. Samoylova and T. Schultz, *PCCP*, 2009, 11, 3927-3934.
29 M. Kunitski, Y. Nosenko and B. Brutschy, *ChemPhysChem*, 2011, 12, 2024-2030.
30 M. Busker, M. Nispel, T. Häber, K. Kleinermanns, M. Etinski and T. Fleig, *ChemPhysChem*, 2008, 9, 1570-1577.
31 J. J. Serrano-Perez, R. Gonzalez-Luque, M. Merchan and L. Serrano-Andres, *J. Phys. Chem. B*, 2007, 111, 11880-11883.
32 M. Etinski, T. Fleig and C. Marian, *J. Phys. Chem. A*, 2009, 113, 11809-11816.
33 P. M. Hare, C. T. Middleton, K. I. Mertel, J. M. Herbert and B. Kohler, *Chem. Phys.*, 2008, 347, 383-392.
34 G. Meijer, M. S. de Vries, H. E. Hunziker and H. R. Wendt, *Appl. Phys. B*, 1990, 51, 395-403.
35 D. Irimia, D. Dobrikov, R. Kortekaas, H. Voet, D. A. van den Ende, W. A. Groen and M. H. M. Janssen, *Rev. Sci. Instrum.*, 2009, 80.
36 T. Ebata, C. Minejima and N. Mikami, *J. Phys. Chem. A*, 2002, 106, 11070-11074.
37 B. C. Dian, A. Longarte and T. S. Zwier, *J. Chem. Phys.*, 2003, 118, 2696-2706.
38 T. Ebata, N. Mizuochi, T. Watanabe and N. Mikami, *J. Phys. Chem.*, 1996, 100, 546-550.
39 T. Walther, H. Bitto, T. K. Minton and J. R. Huber, *Chem. Phys. Lett.*, 1994, 231, 64-69.
40 C. Moller and M. S. Plesset, *Phys Rev*, 1934, 46, 618-622.
41 C. Hattig, *Advances in Quantum Chemistry, Vol 50*, 2005, 50, 37-60.
42 A. Kohn and C. Hattig, *J. Chem. Phys.*, 2003, 119, 5021-5036.
43 C. Hattig, *J. Chem. Phys.*, 2003, 118, 7751-7761.
44 T. H. Dunning, *J. Chem. Phys.*, 1989, 90, 1007-1023.
45 V. Barone, *J. Chem. Phys.*, 2005, 122.
46 J. W. Cooley, *Math Comput*, 1961, 15, 363.
47 B. B. Brady, L. A. Peteanu and D. H. Levy, *Chem. Phys. Lett.*, 1988, 147, 538-543.
48 D. Dougherty, K. Wittel, J. Meeks and S. P. McGlynn, *J. Am. Chem. Soc.*, 1976, 98, 3815-3820.
49 V. Vaquero, M. E. Sanz, J. C. Lopez and J. L. Alonso, *J. Phys. Chem. A*, 2007, 111, 3443-3445.
50 R. N. Casaes, J. B. Paul, R. P. McLaughlin, R. J. Saykally and T. van Mourik, *J. Phys. Chem. A*, 2004, 108, 10989-10996.
51 M. R. Viant, R. S. Fellers, R. P. Mclaughlin and R. J. Saykally, *J. Chem. Phys.*, 1995, 103, 9502-9505.
52 C. Puzzarini, M. Biczysko, V. Barone, I. Pena, C. Cabezas and J. L. Alonso, *PCCP*, 2013, 15, 16965-16975.
53 J. C. Lopez, J. L. Alonso, I. Pena and V. Vaquero, *PCCP*, 2010, 12, 14128-14134.
54 J. C. Lopez, M. I. Pena, M. E. Sanz and J. L. Alonso, *J. Chem. Phys.*, 2007, 126.
55 J. J. Szymczak, M. Barbatti, J. T. S. Hoo, J. A. Adkins, T. L. Windus, D. Nachtigallova and H. Lischka, *J. Phys. Chem. A*, 2009, 113, 12686-12693.
56 H. R. Hudock, B. G. Levine, A. L. Thompson, H. Satzger, D. Townsend, N. Gador, S. Ullrich, A. Stolow and T. J. Martinez, *J. Phys. Chem. A*, 2007, 111, 8500-8508.
57 Z. G. Lan, E. Fabiano and W. Thiel, *J. Phys. Chem. B*, 2009, 113, 3548-3555.
58 D. Nachtigallova, A. J. A. Aquino, J. J. Szymczak, M. Barbatti, P. Hobza and H. Lischka, *J. Phys. Chem. A*, 2011, 115, 5247-5255.